NAL SCIENTIFIC REVIEW
SR-1

APPLICATION OF X-RAY AND ELECTRON SPECTROSCOPY TO MATERIALS SCIENCE

S. RAMASESHAN & T.G. RAMESH

NATIONAL AERONAUTICAL LABORATORY
BANGALORE-17, INDIA

NAL SCIENTIFIC REVIEW
SR-I

APPLICATION OF X-RAY AND ELECTRON SPECTROSCOPY TO MATERIALS SCIENCE

by

S. RAMASESHAN & T.G. RAMESH

ERRATA

Page	Line	Read	For
3	13	eV	ev
3	31	an	en
3	33	Is	Is
6	20	Al ion in Li_2O Al_2O_3	Al ion in Li_2O. Al_2O_3
7	6	$\|\psi(r)\|^2$	$/\psi(r)/^2$

NATIONAL AERONAUTICAL LABORATORY
BANGALORE-17, INDIA

CONTENTS

FIGURES

APPLICATION OF X-RAY AND ELECTRON SPECTROSCOPY * TO MATERIALS SCIENCE

S. RAMASESHAN & T.G. RAMESH

SUMMARY

The basic principles underlying X-ray emission, Auger effect and X-ray absorption are reviewed in this note. The experimental methods of obtaining the energy of binding by the spectroscopy of ejected electrons (ESCA) are presented. The alteration in the energy levels due to covalent and ionic bonding is next discussed. The chemical shifts observed and its uses in the study of bonding, co-ordination, electro-negativity, oxidation states and in organic structure analysis are dealt with briefly with examples. The paper finally deals with the important application of X-ray spectroscopy in the study of band structure of materials and how the energy gaps can be measured. The theory of extended X-ray fine structure is briefly touched upon.

* Talk delivered by Dr. S. Ramaseshan at Chemistry Symposium organised by Bhabha Atomic Research Centre at I.I.T., Madras, on 25th November, 1970.

APPLICATION OF X-RAY AND ELECTRON SPECTROSCOPY* TO MATERIALS SCIENCE

S. RAMASESHAN & T.G. RAMESH

1. X-RAY EMISSION, AUGER EFFECT AND X-RAY ABSORPTION[1]

X-ray Emission :

The deceleration of an incident electron beam by the cloud of electrons of the atoms of the target material results in the continuous X-ray emission spectrum (Bremstralung) having a short wave-length limit. As the tube voltage increases above a certain level, sharp lines characteristic of the target material appear, superposed on the continuous background. The incident electrons create vacant states in the deeper electronic shells of an atom. In this excited atom (ion), an electron may fall from a higher electronic level to the vacant state, the energy difference being converted into an X-ray quantum of frequency, ν, given by $E_2 - E_1 = h\nu$. Mosley, in his classical researches, found a linear relationship between $\sqrt{\nu}$ and Z, the atomic number of the element. On the basis of Bohr's theory of the hydrogen atom, he proposed the formula

$$\nu_{K\alpha} = R_0 (Z-\sigma)^2 \left\{ \frac{1}{1^2} - \frac{1}{2^2} \right\} \qquad (1)$$

where σ is the screening constant. When an electron in the K shell is removed, the electrons in the L shell see the field of the nucleus shielded by the remaining electron of the K shell giving rise to a screening constant, $\sigma \approx 1$ for all elements. $(Z-\sigma)$ is called the effective nuclear charge. The experimental verification of Eq. (1) implies that in X-ray spectra one is essentially concerned with hydrogen like terms. Since the strong lines in the X-ray spectra arise due to transitions in the inner electronic shells, energies of these levels are governed predominantly by the effective nuclear charge so that the elementary Bohr theory is adequate. The transitions between the energy levels are governed by the selection rules $\Delta l = \pm 1$ and $\Delta J = 0, \pm 1$. Thus the transition $L_1 \longrightarrow K$ is forbidden as both these states are spherically symmetric.

* Talk delivered by Dr. S. Ramaseshan at Chemistry Symposium organised by Bhabha Atomic Research Centre at I.I.T., Madras, on 25th November, 1970.

Auger Effect :

An atom in a state of excitation with a vacancy in an inner electronic shell can be de-excited in one of two ways : (a) An electron from a higher shell can fall to this vacant state, the energy difference manifesting itself as an X-ray quantum. (b) The energy difference between the two levels may eject another electron from a higher level of Energy E_3 and impart to it a definite kinetic energy given by

$$E_{Kin} = E_2 - E_1 - E_3$$

These radiationless transitions were first observed by Auger while studying the X-ray fluorescence of argon gas in a cloud chamber. Earlier the Auger effect was thought of as a process of internal conversion *i.e.* first an X-ray quantum is generated which, instead of coming out of the atom, causes an internal photoelectric effect. Such reasoning is found to be incorrect, for, one finds experimentally Auger electrons resulting from forbidden transitions. The Auger transition is now explained in terms of the Coulomb interaction between the two vacancies in different shells [For a detailed treatment of the effect, see Refs (1) and (2)].

X-ray Absorption :

When a beam of X-rays of intensity I_0 traverses a material of thickness x, the emergent intensity I is given by $I = I_0 e^{-\mu x}$ where μ is the linear attenuation coefficient. The decrease in intensity is due to the unmodified and Compton radiation that is scattered away and to the true absorption which is due to the photoelectric ejection of electrons from inner shells. $\mu = \Sigma + \tau$ where Σ and τ represent the scattering and true absorption coefficients respectively. An atom has one K-absorption edge, three L-edges, five M-edges and so on. Experimentally only the position of the K-edge can be determined with high precision so that much of the absorption spectroscopic work is concentrated on the K-absorption edge.

The position of the K-absorption edge depends on whether the element in question is in the form of a gas or a solid and that too whether it is an insulator or in the metallic state. In the case of a gas, the K-edge corresponds to the energy necessary to remove an electron from the K-shell to infinity. The absorption edge in solids will be discussed later.

The energy levels in an atom can be experimentally determined by combining data from X-ray absorption and emission spectroscopy. The position of the K-edge determines the absolute energy of the K-shell and the other levels can be fixed from a knowledge of the characteristic X-ray emission spectra. The wavelength of the X-ray emission lines can be determined to a high degree of accuracy whereas the location of an absorption edge is not so precise.

2. *SPECTROSCOPY OF THE EJECTED ELECTRONS*

Electrons ejected from atoms by photoelectric absorption of X-rays of frequency ν, have kinetic energies, E_{kin}, given by

$$E_{kin} + E_b = h\nu \qquad (2)$$

where E_b is the binding energy of the electron. If E_{kin} could be measured accurately (using a magnetic β-ray spectrometer), the energy of binding, E_b, could be calculated using Eq. (2) and a precise knowledge of the frequency of the incident photon. This electron spectroscopic method[4] which has been pioneered and perfected by K. Siegbahn, provides a direct means of probing the energy levels of atoms and has many advantages over conventional X-ray spectroscopy. This new tool combines the high resolution of X-ray spectroscopy (through a knowledge of the frequency of the X-ray photon) with the highest resolution in β-ray spectroscopy. It is now possible to measure the binding energies of electrons accurate to better than 0.1 ev so that the electron spectroscopic method provides a potential tool to investigate the changes in the binding energy associated with chemical bonding.

A schematic diagram of the apparatus which has been used for electron spectroscopic determinations of binding energies is shown in Fig. 1. Monochromatic X-radiation strikes the specimen (called the converter) and photoelectrons which are ejected are analysed in a β-ray spectrometer. In the permanent magnet spectrograph, the ejected electrons with the same kinetic energy but having an angular divergence in a plane perpendicular to the constant magnetic field can be focussed on the slit system. But in a double-focussing spectrometer[6], both angular as well as space focussing can be achieved if the magnetic induction varies from the symmetry axis as $1/\sqrt{r}$. The energies of the electrons involved in electron spectroscopic measurements lie in the low energy region of 3-10 KeV which corresponds to a magnetic field of about 15 to 17G in spectrographs with the radius of curvature varying from 10 cm to 24 cms. For accurate measurements, therefore, it is essential to maintain a homogeneous magnetic field and the earth's magnetic field has to be compensated using Helmholtz's coils. Further the remnant effects associated with the magnetic materials used in the construction of the spectrograph become serious in the low magnetic field region and hence iron-free spectrometers have been designed[7-10] for accurate energy analysis of the photoelectrons. These low energy electrons are detected in the slit system using a photographic emulsion technique[11].

In electron spectroscopic work, E_b, the binding energy of en electron is defined as the energy required to remove an electron from the shell to the Fermi-level, which could in general be defined as the level whose probability of occupation is 1/2. This definition is valid both for a metal and an insulator. The spectrometer slit system and the specimen are electrically connected so that their Fermi-levels are equalised. Figure 2 gives the energy band scheme of the slit system (metal) and the specimen in the metallic as well as insulating states. The K-absorption edge and the valence band emission spectra of the specimen in both the states are

also shown in the diagram. If ϕ_{sp} is the work-function of the slit system, it is seen from Fig. 2 that E_{kin} as measured at the slit is given by

$$E_{kin} = h\nu - E_b - \phi_{sp} \quad (3)$$

The electron spectrum of a material consists of both the primary photoelectrons and Auger electrons[1,2]. The measurement of the E_{kin} of the Auger electrons also provide information about the energy levels from which they originate. Since the fluorescence yield in low atomic number elements is poor whereas the Auger yield is very much higher, electron spectroscopic method is particularly suitable to probe their energy levels.

3. *EFFECT OF CHEMICAL BONDING ON THE ENERGY LEVELS*

When chemical bonding occurs there is a redistribution of the valence electrons between the atoms. This alters all the energy levels of the atoms although the outer electronic shells are affected most. The energy levels and the wave-functions in a many-electron atom can be evaluated using Hartree's self consistent field method. If $\psi(r)$ represents the wave-function of an electron in a stationary state, then $-e|\psi(r)|^2$ can be considered to be the average charge density due to this electron at a point defined by r. For each wave-function enumerated in Hartree's method, one may plot the radial charge density as a function of r. Figure 4 presents a schematic diagram of the radial charge densities associated with various wave-functions in K^+ ion. One notices that each wave-function is associated with a continuous charge distribution throughout the atom. Thus every electron in the atom contributes to the screening parameter, σ. From the well-known theorem in electrostatics, only the charge distribution within the electronic shell of interest contributes significantly towards this screening parameter. The chemical shifts associated with bond-formation can now be qualitatively understood.

Covalent Bond :

In a covalent bond, the distribution of the valence electrons is altered in such a manner that the probability density for finding them in the region of overlap increases whereas the density within the atomic core decreases. This obviously would result in a reduction of the screening parameter which corresponds to an increase in the effective nuclear charge. Thus the inner electrons become more tightly bound to the nucleus and the binding energies of all the levels move towards the higher energy side. This may be accompanied by another effect caused by the decrease in the atomic volume when bonding takes place. This is mostly found in transition element compounds where a sharp decrease in the interatomic distance occurs with increasing valency. The decrease in the atomic volume is associated with an increase in electron density throughout the atom, i e. σ is enhanced, pushing the energy levels of electrons towards lower energies. Thus the direction of the shift in the energy levels depends on which of these two above effects predominate (Fig. 5).

Ionic Bond :

An ionic bond is characterised by a transfer of charge between the two atoms and the resulting electrostatic interaction between the positive and negative ions. In the case of the positive ion, owing to the removal of an electron, σ decreases, increasing the effective nuclear charge so that the energy levels shift towards the higher energy side. On the other hand, for the negative ion, the energy levels shift towards the lower energy side consequent to the decrease in the effective nuclear charge (Fig. 5).

Partial Ionic Character :

When atoms having different electro-negativities form a chemical bond, the sharing of the valence electrons will not be equal giving a partial ionic character to the bond. According to Pauling, the difference in the electro-negativity between the two atoms is a measure of the ionicity of the bond. Thus, one may associate an effective charge on the atoms involved in the bond which can be estimated using Pauling's criterion[13]. The direction of the shifts in the energy levels for the two atoms may be determined in the manner given for the ionic band.

X-ray emission spectroscopy and ESCA (Electron spectroscopy for chemical analysis) have provided valuable information on the chemical environment of an atom through the measurement of the chemical shifts in the energy levels of the atom. The shift in an emission line corresponds to a difference in the chemical shifts of the two levels involved in the transition. For example, the energy shifts of the K and L levels are of the same order of magnitude, ΔL usually being greater than ΔK leading to a much smaller shift in the position of the K_α emission line. This is in contrast to the ESCA method in which the shifts of each individual level is measured separately. Further in ESCA, the theoretical interpretation of the measured shifts is also simpler in most cases.

4. *CHEMICAL SHIFTS, COORDINATION AND ELECTRONEGATIVITY : EXAMPLES*

Considerable amount of work has been done on the chemical bonding studies using ESCA, X-ray emission and absorption spectroscopy and a detailed account of it can be found in Ref. 4. We shall present only some of them to illustrate some of the broad aspects covered. The photoelectron spectrum exhibiting the chemical shifts in sulphur 2P level[4] in sodium thiosulphate is given in Fig. 6. Sulphur is present in two oxidation states namely -2 and $+6$. These two give clearly resolved peaks, the difference in the binding energy being 6 eV. Some later measurements on the shifts in 1S, 2S and 2P levels[14] in different oxidation states, have shown that the innermost 1S level is affected to a greater extent than the 2S and 2P levels.

The electron spectra of the carbon 1S level in ethanol, ethyl trifluoroacetate and ethyl chloroformate[13] are given in Fig. 7. There are as many peaks in the spectra as the number of chemically non-equivalent carbon atoms. The difference in the binding energy of 1S level between the methyl and methylene carbons is about 1.4 eV in ethanol. The substitution of a

higher electronegative $CF_3C(0)$ group in place of OH group in ethanol affects both the methyl and methylene carbons, their binding energies being shifted towards higher energies. In ethyltrifluoroacetate, if chlorine is substituted for CF_3, the higher electronegativity of the former shifts the 1S level of methylene carbon towards still higher binding energy while there is not much effect on the methyl carbon. The application of this to organic structure analysis is obvious.

The electron spectrum of C1S, Cl 2P and S2P in a series of organic compounds[4] is shown in Fig. 8. The shifts in the binding energy of nitrogen 1S level[13] in various nitrogen compounds has been successfully correlated with the effective charge on the nitrogen atom estimated using Hückel's electronegativity criterion.

5. *COORDINATION NUMBER AND X-RAY EMISSION SPECTROSCOPY*

Some elements of low atomic number like Aluminium and Silicon exhibit a regular dependence of the X-ray emission wavelength on the coordination number of the site occupied. The positions of the Al K_α peaks from clay minerals[15] are compared with these from Al metal. From a prior knowledge of their crystal structures, one may classify the Al K_α peak positions into three broad regions. Structures with the Al ions (a) in tetrahedral sites only exhibit a shift of about 0.25 eV (e.g. Ca0. $Al_2 0_3$, $Na_2 0$. $Al_2 0_3$), (b) in both tetrahedral and octahedral sites as in spinel structures have shifts of about 0.35 eV (e.g. Mullite and β-alumina), (c) in octahedral sites only producing a shift of about 0.5 eV (e.g. Kaolinite, Cryolite). It is interesting that the coordination of Al ion in $Li_2 0$. $Al_2 0_3$ could be deduced to be tetrahedral from these studies. Crystal structure determination of clay minerals is so complex that this method of analysis may prove simpler. It has also the advantage in that the coordination in amorphous substances could also be determined.

In various silicates the position of the Si K_β peak is affected by the nature of the tetrahedral linkage. Since the outer 3P level of silicon is involved in both bond formation and in K_β emission, significant shifts of the peak of this line are observed[16] while K_α is not affected to this extent. For example, a peak shift of -2.7 eV between silicon and α-quartz and about -1.9 eV between stishovite and α-quartz have been measured. Those silicates which have framework tetrahedral linkage give Si K_β peaks close to that of α-quartz while the isolated tetrahedral structures give peaks close to that of Stishovite. The mean Si–0 bond length is characteristic of the kind of tetrahedral linkage present and it has been correlated with the peak positions of the K_β band. It is interesting to note that this method of analysis reveals that SiO film consists of a mixture of silicon and SiO_2, there being no divalent silicon.

In various chlorine compounds, the wavelength of the peak of the $L_{2,3}$ band of chlorine[17] is found to increase as the electronegativity of the metal ion increases. As the electronegativity

of the metal ion decreases imparting more ionic character to the bond, the Cl $L_{2,3}$ band shifts towards higher energies.

6. *ELECTRONIC STRUCTURE OF MATERIALS BY X-RAY SPECTROSCOPY*

X-ray emission spectroscopy has long been recognised as a useful tool to probe the electronic structure of a crystallite material which consists of knowing the spatial distribution i.e. $/\psi(r)/^2$, the energies, E(K) of the valence electrons and the density of states N(E). A determination of E as a function of $\vec{K}$, the wave-vector of the electron, (which in a crystal falls into allowed and forbidden energy bands) provides information about the band structure of the crystal. In a metal, the valence band (conduction band) is partially filled with electrons occupying states upto the Fermi-level while in an insulator the valence band is completely filled (Fig. 9).

The intensity distribution of an emission band is given by $I(E) \alpha P(E) N(E)$ where P(E) is the transition probability. It is now recognised that both these factors are important[18] in determining the emission profile. The matrix element of the transition is given by $M = \int \psi_f^*(r)\, r\, \psi_i(K, r)\, d^3 r$. ψ_i and ψ_f are the initial (inner electron hole + valence electron) and final (valence electron hole) wave functions. In the K-emission spectra, only that portion of ψ_f which overlaps IS wave-function which is highly localised contributes to the above integral. Thus X-rays originate only from these local regions of overlap. X-ray emission spectroscopy can therefore probe only these limited regions in the material. A measurement of I(E) as a function of E involves only one variable and as the electron distributions and energies are in three-dimensional space, it is impossible to obtain a complete electron structure of a material.

Absorption spectroscopy can provide information about the unoccupied electron states in a band. If the element is in the metallic state, then the position of absorption edge corresponds to a removal of the electron from its bound level to the Fermi-level whereas for an insulator, the absorption edge corresponds to an electron removal to the empty states in the next allowed energy band. The valence emission band in an insulator is due to transitions from the filled valence band to the inner vacant states (Fig. 2). Thus a combination of X-ray emission and absorption spectroscopy, in an insulator, can provide a measure of the forbidden energy gap.

The L_{III} emission and absorption edge measurements in transition metal oxides TiO_2 and V_2O_5[19] are given in Fig. 10. These oxides are supposed to contain empty 3d bands and the emission spectra has been interpreted as arising due to crossover transitions i.e. a hole in the L_{III} level of metal ion is filled by, say, the 2P electron of the oxygen ion. This $02P \longrightarrow L_{III}$ transition is normally forbidden (dipole selection rule), but occurs in these cases, probably, due to the strong anion-cation orbital overlap. The forbidden gap corresponds to the energy difference between the empty 3d band of metal ion and the filled 2P oxygen band. The experimental values of the gap width are 3.5 eV for TiO_2 and 3.8 eV for V_2O_5 and these are in good agreement with optical and thermal data.

7. EXTENDED X-RAY FINE STRUCTURE

The absorption spectrum of a substance on the high energy region of the absorption edge exhibits fine structure. Within an energy range of about 30 eV for the ejected electron, it is referred to as Kossel structure and the region extending to about 150 eV is termed Kronig structure. Extended X-ray Fine Structure (EXFS) is exhibited by both crystalline and amorphous materials possessing short-range order. Lytle has given a particle in a box model[20] to explain this fine structure, according to which, the interaction of the ejected electron wave with the coordination polyhedra is of primary importance. Using the Wigner-Seitz method, one can then solve the allowed energy values of the ejected electron. An absorption maximum in the fine structure, occurs whenever, E, the energy of the ejected electron satisfies the equation

$$E = \frac{h^2}{8 m \gamma_s^2} \cdot Q$$

where Q represents the zero-roots of the half-order Bessel function which appears in the radial part of the solution of the Schrödinger wave equation; γ_s is the radius of the equivalent sphere. The Kronig structure and E vs Q plot for gaseous $GeBr_4$ is given in Fig. 11. The slope yields γ_s, from which one can obtain the size of the coordination polyhedra. For $GeBr_4$, $\gamma_s = 2.29$ Å, in very good agreement with the Ge-Br distance of 2.32 Å. Experimental measurements of the fine structure in germanium, Ion, copper and some compounds of Yttrium[21] confirm the general validity of Lytle's model.

8. CONCLUSION

The acquisition of an electron microprobe analyser attachment to our electron microscope prompted us to study this subject. We also felt that this review paper may bring out the invaluable uses of ESCA in chemistry and chemical physics so that research workers in BARC with their tradition of instrumentation may launch on a building programme of ESCA β-ray spectrometers.

REFERENCES

1. Compton, A.H. & Allison, S.K., *X-rays in theory and experiment* (Van Nostrand Co.), 1935.
2. Burhop, E.H.S., *The Auger effect and other radiationless transitions* (Cambridge University Press, London), 1952.
3. Assad, W.N. & Burhop, E.H.S., *Proc. Phys. Soc.*, **71** (1958) 362.
4. Siegbahn, K., *et al; Ann. Phys.*, **t.3 No.5** (1968) 281–329.
5. Fahlman, A. & Siegbahn, K., *Arkiv Fysik*, **32** (1966) 111.
6. Siegbahn, K., *Alpha, Beta and Gamma-ray spectroscopy*, Chapter III, Ed. K. Siegbahn (North Holland Publ. Co., Amsterdam), 1965.
7. Siegbahn, K., *et al; Nucl. Instr.*, **27** (1964) 173.

8. Fahlman, A., *et al; Arkiv Fysik*, **31** (1966) 479.
9. Karlsson, S.E., *et al; Arkiv Fysik*, **38** (1967) 341.
10. Karlsson, S.E., *et al; Nucl. Phys.*, **89** (1966) 513.
11. Carlsson, R., *et al; Arkiv Fysik*, **32** (1966) 99.
12. Bergstrom, I., *et al; Alpha, Beta and Gamma-ray spectroscopy*, Ed. K. Siegbahn, Vol. 2 (North Holland Publ. Co., Amsterdam), 1523.
13. Nordberg, R., *Advances in X-ray Analysis*, **13** (Plenum Press), 391–405.
14. Fahlman, A., *et al; Nature*, **210** (1966) 4.
15. Day Delbert, E., *Nature*, **200** (1963) 649.
16. White, E.W., *Advances in X-ray Analysis*, **9** (Plenum Press), 394.
17. Fischer, W.D. & Baun, L.W., *Advances in X-ray Analysis*, **9** (Plenum Press), 338.
18. Nagel, D.J., *Advances in X-ray Analysis*, **13** (Plenum Press), 182–236.
19. Fischer, D.W., *Advances in X-ray Analysis*, **13** (Plenum Press), 171.
20. Lytle, F.W., *Advances in X-ray Analysis*, **9** (Plenum Press), 399.
21. Bhide, V.G. & Bhat, N.V., *J. Chem. Phys.*, **48** (1968) 3103.

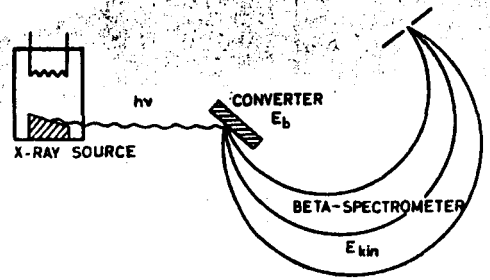

Fig. 1 - Schematic diagram of ESCA apparatus

Fig. 2 - Energy level diagram of specimen in the metallic and insulating states with the transitions corresponding to the K-absorption edge and the valence band emission. The levels of the electrically connected slit system and the quantities E_b, E_{kin} and ϕ_{sp} of relation (3) are also shown.

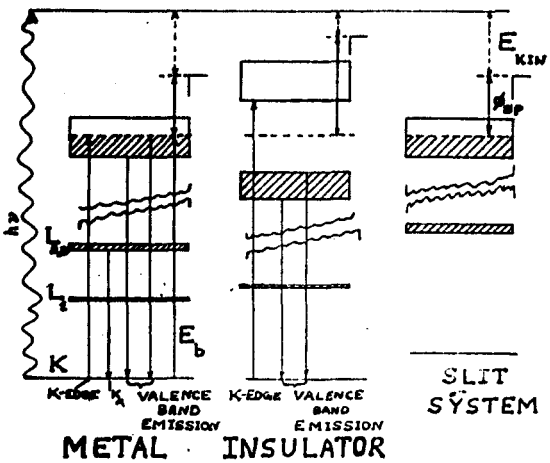

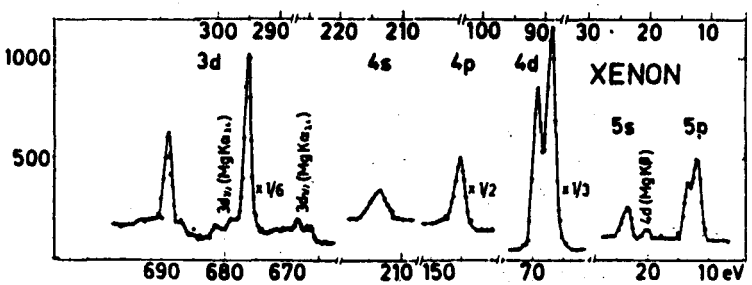

Fig. 3 - Electron spectrum of xenon

Fig. 4 Radial charge densities in K^+ ion.

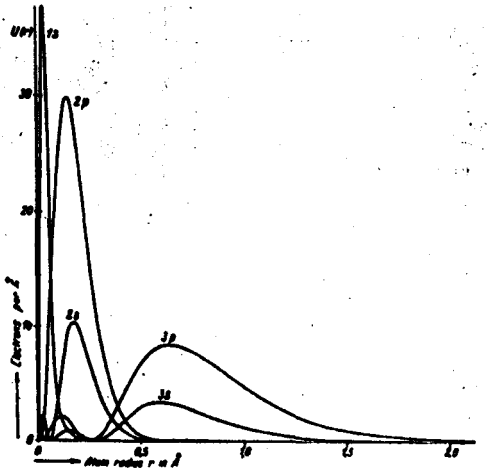

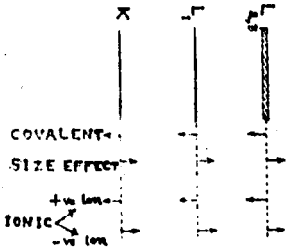

Fig. 5 - Direction of the chemical shifts in energy levels, for covalent bonding size effect and ionic bonding

Fig. 6 - The chemical shifts of the 2p level of sulphur in two different oxidation states (-2 and +6) in $Na_2S_2O_3$.

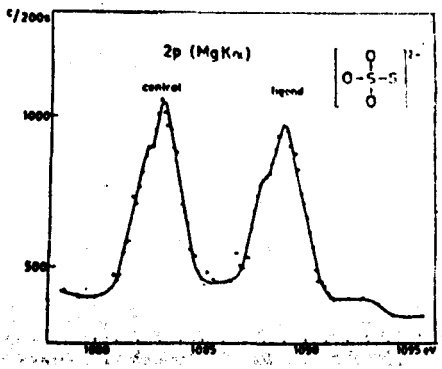

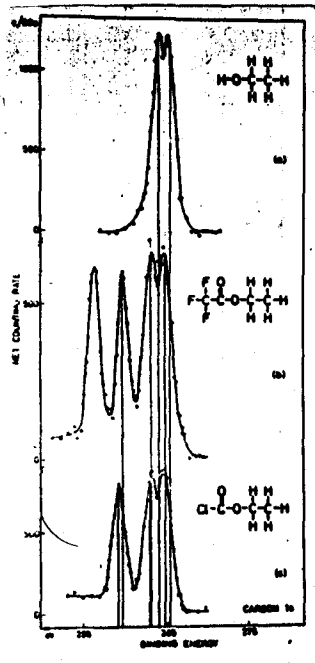

Fig. 7 - Electron spectrum of carbon IS level in ethanol and its derivatives. The shifts in the binding energy of IS level towards higher energy side with the substitution of a higher electro-negative group can be clearly seen.

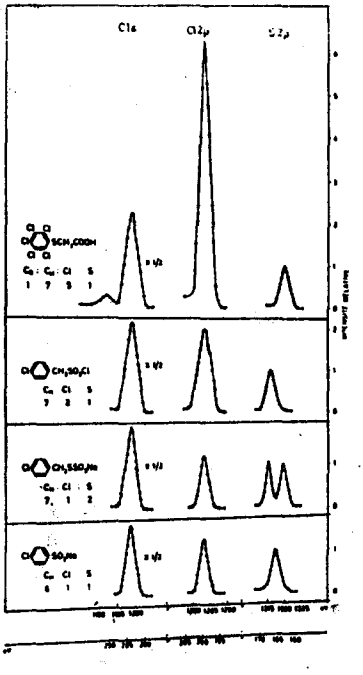

Fig. 8 - The use of ESCA in organic structure analysis.

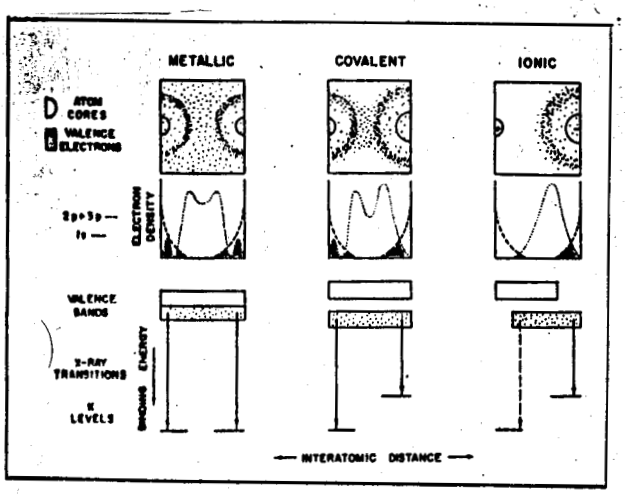

Fig. 9 - Valence electron distributions between atoms in metallic, covalent and ionic bonding. The hatched regions indicate regions of electron density overlap. The K-spectra arising due to these local regions of overlap are also indicated.

Fig. 10 - L_{III} emission and absorption spectra in TiO and V_2O_5

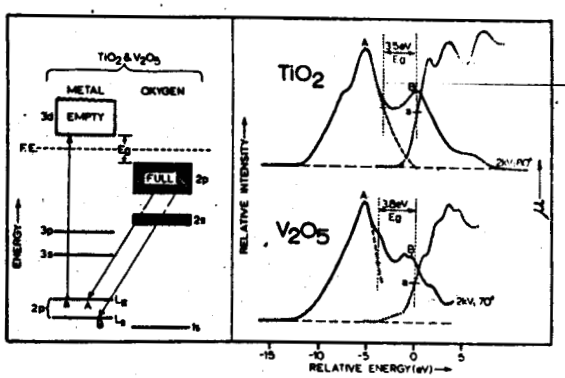

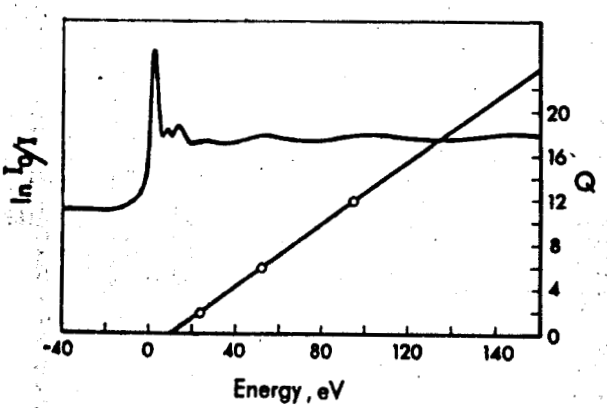

Fig. 11 - Extended X-ray fine structure and E vs Q plot in gaseous $GeBr_4$